RBFNN-Based Consensus Control of Vehicle Platoon With an Adaptive Event-Triggered Mechanism Under DoS Attacks

Xiaoping Zhao, Junyao Ma, Jinliang Liu, *Senior Member, IEEE*, and Lijuan Zha, *Senior Member, IEEE*

***Abstract*—Vehicle platoon is an essential subject in research on intelligent transportation and autonomous driving. Current control systems frequently rely on accurate feedback linearization, which overlooks denial-of-service (DoS) attacks and assumes full parameter information, assumptions that are rarely realized in environments that are noisy and prone to disturbances. The communication topology is described as a directed graph with a spanning tree in this work, which develops an adaptive distributed control framework for uncertain nonlinear vehicle platoons under DoS attacks. The unknown nonlinear dynamics are modeled using radial basis function neural networks (RBFNNs), and coordinated platoon behavior is achieved by developing an adaptive backstepping control approach. To reduce unnecessary control updates, two Zeno-free event-triggered techniques are also presented. Practical consensus is ensured by Lyapunov-based analysis, and simulation results show that string stability is preserved under two-predecessor-following (TPF) and bidirectional (BD) topologies—even when the DoS attack rate hits 70%.**

***Index Terms*—Denial-of-service (DoS) attacks, vehicle platoon, adaptive control event-triggered mechanism, RBF neural network.**

I. Introduction

As AUTONOMOUS-DRIVING technology and intelligent transportation systems (ITS) advance quickly, connected and autonomous vehicles (CAVs) have become essential tools for reducing crash rates, fuel consumption, and traffic congestion. CAV-related research has attracted significant attention in recent years [1], [2], [3], covering perception, communication, and data analytics. Among various applications, platoon control has drawn particular scholarly interest [4], [5] because of its high research value and wide range of potential applications. Stability, safety, and network security are ongoing research concerns since platoons rely on wireless vehicle-to-vehicle (V2V) communications to maintain mandated distances and speed consensus, yet dependable operation still requires highly reliable communication and sophisticated control.

Received 25 July 2025; revised 13 October 2025; accepted 31 December 2025. Date of publication 12 January 2026; date of current version 24 June 2026. This work was supported by the National Natural Science Foundation of China under Grant 62373252. The review of this article was coordinated by Prof. Hongbo Jiang. *(Corresponding authors: Xiaoping Zhao; Jinliang Liu.)*

Xiaoping Zhao, Junyao Ma, and Jinliang Liu are with the School of Computer Science, Nanjing University of Information Science and Technology, Nanjing 210044, China (e-mail: zxp@nuist.edu.cn; mjunyao202507@163.com; liujinliang@vip.163.com).

Lijuan Zha is with the School of Science, Nanjing Forestry University, Nanjing 210037, China (e-mail: zhalijuan@vip.163.com).

Digital Object Identifier 10.1109/TVT.2026.3651490

However, successful platoon operation requires advanced control algorithms and highly reliable communication, posing challenges in stability, safety, and robustness. The majority of controllers in use today are predicated on feedback linearization [6], [7] and presume full model parameter knowledge. They frequently overlook measurement noise and outside disruptions, which is impractical in real-world situations that are nonlinear and vulnerable to attacks. Zhao et al. [8] proposed a distributed adaptive cruisecontrol strategy robust to packet loss, delays, and disruptions, but it remains linear and lacks flexibility for nonlinear dynamics. Internal stability [9], [10], which ensures that each vehicle's state converges to its reference trajectory, and string stability [11], [12], which inhibits disturbance amplification along the vehicle string, are two scientific pillars of platoon control. Recent work has extended to backstepping, fuzzy control, and model predictive control (MPC). Yu et al. [13] linearized vehicle dynamics into a bilinear form and applied linear MPC with path constraints for smooth steering and low yaw-rate errors. Wei et al. [14] proposed an online RBFNN fuzzy controller with adaptive error restrictions to handle nonlinearities and dead zones, ensuring asymptotic and string stability, while Chen et al. [15] combined event-triggering, a state observer, and adaptive backstepping to reduce communication load while ensuring bounded signal convergence. While adaptive controllers like that of Zhu et al. [12] have guaranteed stability for specific topologies, many existing methods still struggle with nonlinear uncertainties, high update rates, and malicious cyber-attacks. In practice, DoS attacks can severely compromise platoon safety by delaying packets, enlarging gaps, and disrupting speed coordination [16], [17]. Although robust distributed strategies exist for large platoons, static attack-performance maps and rule-based filters assume stationary attack patterns and fail against unpredictable adversaries [16], [18], [19]. To better capture the stochastic nature of DoS, Liu et al. [20] modeled them as Bernoulli processes. Building on this, we incorporate external disturbances and model DoS attacks as a Bernoulli process to enhance robustness against unknown perturbations and simultaneous stochastic attacks. To handle unmodeled nonlinearities (dead zones, aerodynamic drag), we use neural network approximators. We adopt RBFNNs for online approximation because their Gaussian local bases and linear-in-parameters adaptation enable Lyapunov-stable fast updates. Compared with Chebyshev functional-link networks using global Chebyshev expansions (global coupling and order tuning) [21], RBFNNs are more local and responsive for real-time control under bandwidth/DoS limits, with platooning evidence supporting this choice [22], [23]. Prior studies often neglect acceleration control, focus on second-order models, or lack real-time implementation. Event-triggered control (ETC) mitigates bandwidth usage by updating only when necessary, with periodic, static-threshold, and dynamic-threshold schemes reported [24], [25], [26], [27], while Hu et al. [28] presented a Zenofree selftriggered policy that accounts for channel conditions and traffic characteristics. Despite recent advancements in event-triggered distributed control for nonlinear vehicle platoons [29], [30], [31], ETC's potential for nonlinear platoons under stochastic DoS attacks is still largely unrealized, despite its widespread use in multi-agent coordination.

In this paper, we present an adaptive distributed control framework for nonlinear vehicle platoons under DoS attacks. By integrating online RBFNNs, recursive backstepping, and a Zeno-free dual-mode event-triggered mechanism, the strategy ensures spacing and speed consensus. Results across bidirectional (BD) and TPF topologies confirm that string stability and robust performance are maintained even under random packet dropouts.

The main contributions of this paper are:

1) Unlike prior work that ignores cyber risks or assumes fixed attack patterns [12], [16], [19], we incorporate DoS attacks into string- and internal-stability analysis. Modeling attacks as a Bernoulli process yields a unified probability-based stability criterion that reflects practical random packet dropouts.
2) We develop a Zeno-free dual-mode triggering mechanism that balances control accuracy and bandwidth, replacing static, periodic, or single-threshold triggers [24], [25], [26]. The thresholds adapt to attack intensity—tightening in benign intervals to improve tracking and loosening under high DoS to preserve the channel.
3) Unknown nonlinear vehicle dynamics are approximated online by an RBFNN, where only one scalar weight per vehicle is updated [12]. This design reduces computational load and communication latency compared to multi-parameter methods.

The paper is organized as follows: Section II–IV present the problem formulation, main theoretical results, and simulation studies, respectively. Section V concludes the paper.

II. Preliminaries

A. Notations

$\mathcal{N}$ and $\mathcal{N}_0$ are defined as $\mathcal{N}=\{1,2,\ldots,N\}$ and $\mathcal{N}_0=\{0,1,2,\ldots,N\}$, respectively. The set of real numbers is denoted by $\mathbb{R}$, with $\mathbb{R}+$ specifically representing the set of positive real numbers. The set of n-dimensional vectors is denoted by $\mathbb{R}^n$, while $\mathbb{R}^{m\times n}$ represents the set of $m\times n$-dimensional matrices. $\lambda_{\min}(A)$ stands for the minimum eigenvalue of A.

B. System Model

In a formation of $N+1$ connected autonomous vehicles, indexed from 0 to N, each follower i operates under a third-order nonlinear model with parametric uncertainty [32].

$$\begin{cases}\dot{p}_i(t)=v_i(t)\\ \dot{v}_i(t)=a_i(t)\\ \dot{a}_i(t)=u_i^d(t)+d_i(t)+f\{p_i(t),v_i(t),a_i(t)\}\end{cases} \tag{1}$$

where $p_i(t),v_i(t),a_i(t)\in R$ denote the position, velocity, and acceleration of the $i-$th vehicle, respectively. The disturbance term $d_i(t)$ is assumed to be bounded such that $d_i(t)\le\bar{d}$, where $\bar{d}$ denotes a given positive constant. $u_i^d(t)$ denotes the control input of the $i-$th vehicle.

Assumption 1: The state vector $[p_i(t),v_i(t),a_i(t)]^T$ for the i-th vehicle is restricted to a compact set Ω_i. For a given constant $\bar{\xi}$, we consider the subset $\Omega_i\subset\mathbb{R}^3$ defined by all vectors $[p_i(t),v_i(t),a_i(t)]^T$ that satisfy $p_i^2(t)+v_i^2(t)+a_i^2(t)\le\bar{\xi}$. The function $f(p_i(t),v_i(t),a_i(t))$ is continuous but remains unknown throughout this domain.

Specifically, the behavior of the leader vehicle can be modeled as follows:

$$\begin{cases}\dot{p}_0(t)=v_0(t)\\ \dot{v}_0(t)=a_0(t)\\ \dot{a}_0(t)=u_0(t)\end{cases} \tag{2}$$

where $u_0(t)$ represents the reference input used to regulate the leader vehicle so that its velocity tracks $v_0(t)$.

C. Preliminary Concepts

In this work, follower communication is modeled by a directed graph $\mathcal{G}=\{\mathcal{V},\mathcal{E},\mathcal{A}\}$, where $\mathcal{A}=[a_{ij}]\in\mathbb{R}^{N\times N}$ is the adjacency matrix with $a_{ij}>0$ if $(i,j)\in\mathcal{E}$ (information from j to i), and $a_{ij}=0$ otherwise. The neighbor set of node i is $\mathbb{N}i=j\mid(i,j)\in\mathcal{E}$. The Laplacian matrix $\mathcal{L}=[l_{ij}]$ is defined as

$$l_{ij}=\begin{cases}\sum_{j\neq i}a_{ij}, & i=j\\ -a_{ij}, & j\neq i.\end{cases} \tag{3}$$

The leader's influence on the followers is encoded using a diagonal matrix, $\mathcal{K}=\mathrm{diag}\{k_1,\ldots,k_N\}\in\mathbb{R}^{N\times N}$. For each agent i, the corresponding leader-accessible set is defined as follows:

$$\mathbb{K}_i=\begin{cases}0, & \text{if } k_i\neq 0\\ \varnothing, & \text{others.}\end{cases} \tag{4}$$

The set $\mathbb{I}_i$ is given by $\mathbb{N}_i\cup\mathbb{K}_i$, and we denote $\mathcal{H}=\mathcal{L}+\mathcal{K}$.

Assumption 2: The vehicle platoon's network structure includes a spanning tree with the leader node as its root.

This assumption underpins cooperative platoon control. A directed spanning tree guarantees that the leader's state reaches all followers [33], [34], ensuring $\mathcal{L}+\mathcal{K}$ has positive eigenvalues—critical for position and velocity consensus.

Assumption 3 (Stochastic DoS process [20]): For each follower i, let the binary random variable $\alpha_i(t)\in\{0,1\}$ denote packet availability:

$$\alpha_i(t)=\begin{cases}0, & \text{if DoS attacks are active at time } t\\ 1, & \text{otherwise.}\end{cases} \tag{5}$$

1) *Independence:* The sequence $\{\alpha_i(t)\}_{t\geq 0}$ is independent and identically distributed and independent of the system state.
2) *Success probability:* $\Pr\{\alpha_i(t)=1\}=\bar{\alpha}_d$, or, equivalently $\mathbb{E}\{\alpha_i(t)\}=\bar{\alpha}_d$, where $\bar{\alpha}_d\in(0,1)$ is the packet-success rate (so the DoS packet-loss rate is $1-\bar{\alpha}_d$).

Modeling DoS attacks as a Bernoulli process effectively captures random packet dropouts from interference or contention [17], [20], [35]. However, it cannot represent periodic or burst attacks where drop events are not i.i.d., and it assumes a known success probability $\bar{\alpha}_d$, which may require online estimation. Extending to time-correlated and strategic attack patterns is a promising research direction.

Lemma 1 [36]: Given Assumption 2, it holds that $\lambda_{\min}(\mathcal{L}+\mathcal{K})>0$.

Any continuous function $f(x_1,x_2,\ldots,x_m)$ defined on a compact set $\Omega\subset\mathbb{R}^m$ can be represented using an RBFNN as

$$f(X)=\hat{\sigma}^T\Xi(X)+h(t) \tag{6}$$

where $X=[x_1,x_2,\ldots,x_m]^T$, $\Xi(X)$ is the RBF basis vector, $\hat{\sigma}$ denotes the weight vector, and $h(t)$ is the approximation error. The RBF basis function is

$$s_l(X)=\exp\left[-\frac{(X-\mu_l)^T(X-\mu_l)}{\phi_l^2}\right] \tag{7}$$

where μ_l is the center and ϕ_l the width of the l-th neuron.

Lemma 2 [37]: Let $f:\Omega\subset\mathbb{R}^m\to\mathbb{R}$ be continuous. For any $\epsilon>0$, there exists an RBF neural network such that

$$\sup_{X\in\Omega}\left|f(X)-W^{*T}S(X)\right|<\varepsilon \tag{8}$$

where $S(X)=[s_1(X),\ldots,s_n(X),1]^T$, and $W^*\in\mathbb{R}^{n+1}$ denotes the optimal weights.

Lemma 3: For any $x_1,x_2\in\mathbb{R}_+$ and positive constants p,q satisfying $\frac{1}{p}+\frac{1}{q}=1$, Young's inequality holds.

Lemma 4 [38]: Given $\nu>0$ and any real β, the function $\tanh(\cdot)$ fulfills the inequality below.

$$|\beta|-\beta\tanh\left(\frac{\beta}{\nu}\right)\in[0,0.2785\nu]. \tag{9}$$

Lemma 5 [39]: Suppose $V(t)\geq 0$ for all $t\geq 0$ and $V(0)$ is bounded. If V satisfies $\dot{V}(t)\leq-\rho V(t)+\xi$, where $\rho,\xi>0$, then

$$V(t)\leq\frac{\xi}{\rho}+\left(V(0)-\frac{\xi}{\rho}\right)e^{-\rho t}. \tag{10}$$

D. Control Targets

The main goal of platoon control is to guarantee that each follower preserves a specified spacing relative to its preceding vehicle, while all vehicles maintain consistent speed. The inter-vehicle spacing, considered as the output of the dynamic model in (1), is defined as

$$L_i(t)=p_i(t)-p_{i-1}(t)+l_{i-1} \tag{11}$$

where l_{i-1} represents the length of the $(i-1)$-th vehicle and $i\in\mathcal{N}$.

In this work, a constant distance (CD) spacing policy is adopted, where the desired spacing between vehicle $i-1$ and vehicle i is defined as $L_i^d=d_i$. Here, d_i denotes the prescribed target gap for each $i\in\mathcal{N}$.

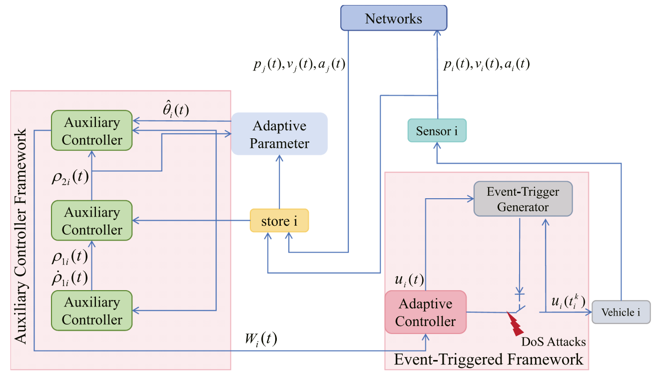

Fig. 1. Adaptive event-triggered control under DoS attacks.

$$L_i^d(t)=d_i. \tag{12}$$

Definition 1: The following presents the practical consensus criterion for the platoon:

$$\begin{cases}\lim_{t\to\infty}\|L_i(t)-L_i^d(t)\|\leq\Delta_1\\ \lim_{t\to\infty}\|v_i-v_{i-1}\|\leq\Delta_2\end{cases} \tag{13}$$

where $\Delta_1\geq 0,\Delta_2\geq 0$ are constants.

In particular, setting $\Delta_1=0$ and $\Delta_2=0$ yields asymptotic consensus as a special case of practical consensus.

String stability is an essential property in platoon control, guaranteeing that disturbances in inter-vehicle spacing are not amplified as they propagate through the vehicle string.

Definition 2: As noted in [40], the string stability of a vehicle platoon is defined by the following condition:

$$e_1(t)\geq e_2(t)\geq\cdots\geq e_{N-1}(t)\geq e_N(t), \tag{14}$$

that is

$$H_i(s)=\left|\frac{E_i(s)}{E_{i-1}(s)}\right|\leq 1,\quad i=2,\ldots,N. \tag{15}$$

String stability for a vehicle platoon is defined mathematically as follows: where $e_i(t)=L_i(t)-y_i^d(t)$ represents the spacing error for the $i-$th vehicle, and $E_i(s)$ denotes the Laplace transform of $e_i(t)$.

For simplicity, the notation (t) will be omitted throughout the paper whenever no confusion arises.

III. Adaptive Event-Based Distributed Control

This section introduces an adaptive distributed event-triggered control scheme using RBFNNs and a backstepping design to achieve consensus in nonlinear vehicle platoons under DoS attacks, with the complete framework shown in Fig. 1.

Remark 1: The event-trigger generator is a logical decision-making module responsible for continuously monitoring the defined event-triggering condition. It compares the current state-dependent control law $W_i(t)$ with the last transmitted control input $u_i(t_i^k)$ and generates a trigger signal only when the error between them exceeds the prescribed threshold.

A. Adaptive Distributed Event-Triggered Control Framework

For each $i \in N$, the coordinates are transformed as

$$\begin{cases} m_{1i} = -k_i(p_i - p_0 + d_{i0}) + \sum_{j\in\mathbb{I}_i} (a_{ij}(p_i - p_j + d_{ij})) \\ m_{2i} = v_i - \rho_{1i} \\ m_{3i} = a_i - \rho_{2i}. \end{cases} \tag{16}$$

The distance offset between vehicle i and j is computed as the cumulative sum of desired gaps and preceding vehicle lengths between them, with a positive or negative sign depending on their relative positions:

$$d_{ij} = \sum_{k=\min(i,j)+1}^{\max(i,j)} (d_k + l_{k-1}) \cdot \mathrm{sgn}(j-i) \tag{17}$$

Moreover, ρ_{1i} and ρ_{2i} are generated as the outputs of first-order filters, with κ_{1i} and κ_{2i} serving as their respective inputs. The precise definitions of κ_{1i} and κ_{2i} will be provided in a subsequent section.

Remark 2: The signals $\dot{\kappa}_{1i}$ and $\dot{\kappa}_{2i}$ are obtained by first-order filtering to ensure the continuity necessary for RBFNNs, as event-triggered control can cause discontinuities.

In the following analysis, the event-triggered condition involves several absolute value terms, typically handled by the discontinuous sign function, which may cause chattering. To avoid this, we adopt the smooth approximation proposed in [41], defined as

$$X(z_{li}) = \begin{cases} \dfrac{m_{li}}{|m_{li}|}, & |m_{li}| \geq \zeta_{li} \\ \dfrac{m_{li}}{|m_{li}| + (\zeta_{li}^2 - |m_{li}|^2)^{5-i}}, & |m_{li}| < \zeta_{li}, \end{cases} \tag{18}$$

$$\beta_{li} = \begin{cases} 1, & |m_{li}| \geq \zeta_{li} \\ 0, & |m_{li}| < \zeta_{li} \end{cases} \tag{19}$$

where ξ_{li} denotes a prescribed positive constant. Then,

$$\begin{aligned} \beta_{li} X(m_{li}) m_{li} &= \begin{cases} m_{li}, & m_{li} \geq \zeta_{li} \\ 0, & m_{li} \in (-\zeta_{li}, \zeta_{li}) \\ -m_{li}, & m_{li} \leq -\zeta_{li} \end{cases} \\ &= \beta_{li}|m_{li}|. \end{aligned} \tag{20}$$

Define $x_{k'i} \triangleq \rho_{k'i} - \kappa_{k'i}$ $(k' = 1, 2)$, with $\rho_{k'i}$ given by:

$$\tau_{k'i}\dot{\rho}_{k'i} + \rho_{k'i} = \kappa_{k'i} \tag{21}$$

where $\tau_{k'i}$ denotes a positive constant.

The following section details the threestep backstepping procedure for designing the auxiliary controller.

Procedure 1: Considering the first error variable m_{1i}, the subsequent error variable m_{2i} is treated as a virtual control input, for which a virtual control law κ_{1i} is designed to stabilize the m_{1i} subsystem. The Lyapunov function is selected as follows:

$$V_{1i} = \frac{1}{2}\beta_{1i} m_{1i}^2. \tag{22}$$

The time derivative of V_{1i} is computed as

$$\begin{aligned} \dot{V}_{1i} &= \beta_{1i} m_{1i}(v_i + \dot{m}_{1i} - v_i) \\ &= \beta_{1i} m_{1i}(m_{2i} + \kappa_{1i} + x_{1i} + \dot{m}_{1i} - v_i). \end{aligned} \tag{23}$$

To proceed, define the virtual control input κ_{1i} such that

$$\kappa_{1i} = -\left(h_{1i} + \frac{5}{4}\right) m_{1i} - X(m_{1i})(\zeta_{2i} + 1) - \dot{m}_{1i} + v_i. \tag{24}$$

By designing the virtual control law κ_{1i} in this manner, the $\dot{V}_{1i}$ contains the negative definite term. This stabilizes the subsystem with respect to m_{1i} and lays the foundation for the subsequent design step. By applying Young's inequality, we have

$$\begin{aligned} \dot{V}_{1i} \leq &-\left(h_{1i} + \frac{5}{4}\right)\beta_{1i} m_{1i}^2 + \beta_{1i} m_{1i}^2 + \frac{1}{4}x_{1i}^2 \\ &+ \beta_{1i}\left(|m_{1i}||m_{2i}| - |m_{1i}|(\zeta_{2i} + 1)\right) \\ = &-\left(h_{1i} + \frac{1}{4}\right)\beta_{1i} m_{1i}^2 + \beta_{1i}|m_{1i}|\left(|m_{2i}| - (\zeta_{2i} + 1)\right) \\ &+ \frac{1}{4}x_{1i}^2. \end{aligned} \tag{25}$$

From the definition of x_{1i} and (20), it follows that:

$$\dot{x}_{1i} = \dot{\rho}_{1i} - \dot{\kappa}_{1i} = -\frac{x_{1i}}{\tau_{1i}} - \dot{\kappa}_{1i}, \tag{26}$$

$$\left|\dot{x}_{1i} + \frac{x_{1i}}{\tau_{1i}}\right| \leq g_{1i}(\dot{m}_{1i}, \ddot{m}_{1i}, \dot{v}_i) \tag{27}$$

where the virtual control law κ_{1i} and its derivative are continuous functions of bounded signals, its derivative is necessarily bounded on a compact set; g_{1i} represents this upper bound. Substituting into (26) and (27), we further derive

$$\left|\dot{x}_{1i} + \frac{x_{1i}}{\tau_{1i}}\right| = |\dot{\kappa}_{1i}| \leq g_{1i}(m_{1i}, \dot{m}_{1i}, v_i). \tag{28}$$

From Young's inequality, we have

$$x_{1i}\dot{x}_{1i} \leq -\frac{x_{1i}^2}{\tau_{1i}} + x_{1i}^2 + \frac{1}{4}g_{1i}^2. \tag{29}$$

Taking the expection of $\dot{V}_{1i}$, we have $\mathbb{E}\{\dot{V}_{1i}\} = \dot{V}_{1i}$.

$$\begin{aligned} \mathbb{E}\{\dot{V}_{1i}\} \leq &-\left(h_{1i} + \frac{1}{4}\right)\beta_{1i} m_{1i}^2 + \beta_{1i}|m_{1i}|\left(|m_{2i}| - (\zeta_{2i} + 1)\right) \\ &+ \frac{1}{4}x_{1i}^2. \end{aligned} \tag{30}$$

Procedure 2: We treat m_{3i} as a new virtual control input and design the virtual control law κ_{2i} for the augmented subsystem comprising both m_i and m_{2i}. V_{2i} is specified for Lyapunov analysis as

$$V_{2i} = \frac{1}{2}\beta_{2i} m_{2i}^2 + V_{1i}. \tag{31}$$

By computing its time derivative, we obtain

$$\begin{aligned} \dot{V}_{2i} &= \beta_{2i} m_{2i}(\dot{v}_i - \dot{\rho}_{1i}) + \dot{V}_{1i} \\ &= \beta_{2i} m_{2i}(m_{3i} + \kappa_{2i} + x_{2i} - \dot{\rho}_{1i}) + \dot{V}_{1i}. \end{aligned} \tag{32}$$

Define the virtual control input κ_{2i} as

$$\kappa_{2i} = -\left(h_{2i} + \frac{9}{4}\right) m_{2i} - X(m_{2i})(\zeta_{3i} + 1) + \dot{\rho}_{1i}. \tag{33}$$

This step stabilizes the m_{2i} subsystem based on the established stability of m_{1i}, as shown by $\dot{V}_{2i}$ in (34).

$$\begin{aligned}
\dot{V}_{2i} \leq{}& \beta_{2i} m_{2i}\left(m_{3i} - \left(h_{2i} + \frac{9}{4}\right) m_{2i} - X(m_{2i})(\zeta_{3i} + 1)\right.\\
&\left.+x_{2i}\right) - \left(h_{1i} + \frac{1}{4}\right)\beta_{1i} m_{1i}^2 + \beta_{1i}|m_{1i}|\left(|m_{2i}| - (\zeta_{2i}\right.\\
&\left.+1)\right) + \frac{1}{4}x_{1i}^2\\
\leq{}& -\left(h_{2i} + \frac{9}{4}\right)\beta_{2i} m_{2i}^2 + \beta_{2i}|m_{2i}|\left(|m_{3i}| - (\zeta_{3i} + 1)\right)\\
&+ \beta_{2i} m_{2i}^2 - \left(h_{1i} + \frac{1}{4}\right)\beta_{1i} m_{1i}^2 + \beta_{1i}|m_{1i}|\left(|m_{2i}|\right.\\
&\left.-(\zeta_{2i} + 1)\right) + \frac{1}{4}x_{2i}^2 + \frac{1}{4}x_{1i}^2\\
={}& -\left(h_{2i} + \frac{1}{4}\right)\beta_{2i} m_{2i}^2 + \beta_{2i}|m_{2i}|\left(|m_{3i}| - (\zeta_{3i} + 1)\right)\\
&- h_{1i}\beta_{1i} m_{1i}^2 + H_{2i} + \frac{1}{4}x_{2i}^2 + \frac{1}{4}x_{1i}^2
\end{aligned} \tag{34}$$

where $H_{2i} = -\frac{1}{4}\beta_{1i} m_{1i}^2 - \beta_{2i} m_{2i}^2 + \beta_{1i}|m_{1i}|(|m_{2i}| - (\zeta_{2i} + 1))$. Applying Young's inequality, it can be shown that

$$\begin{aligned}
H_{2i} ={}& -\frac{1}{4}\beta_{1i} m_{1i}^2 - m_{2i}^2 + \beta_{1i}|m_{1i}||m_{2i}| - \beta_{1i}|m_{1i}|(\zeta_{2i} + 1)\\
\leq{}& -\frac{1}{4}\beta_{1i} m_{1i}^2 - m_{2i}^2 + \frac{1}{4}\beta_{1i} m_{1i}^2 + m_{2i}^2\\
&- \beta_{1i}|m_{1i}|(\zeta_{2i} + 1)\\
={}& -\beta_{1i}|m_{1i}|(\zeta_{2i} + 1)\\
\leq{}& 0.
\end{aligned} \tag{35}$$

Consequently, we have $H_{2i} \leq 0$. This leads to the following result:

$$\begin{aligned}
\dot{V}_{2i} \leq{}& -\left(h_{2i} + \frac{1}{4}\right)\beta_{2i} m_{2i}^2 + \beta_{2i}|m_{2i}|\left(|m_{3i}| - (\zeta_{3i} + 1)\right)\\
&- h_{1i}\beta_{1i} m_{1i}^2 + \frac{1}{4}x_{1i}^2 + \frac{1}{4}x_{2i}^2.
\end{aligned} \tag{36}$$

Similar to the derivation of x_{1i}, we can obtain that

$$\left|\dot{x}_{2i} + \frac{x_{2i}}{\tau_{2i}}\right| \leq |g_{2i}(m_{2i}, \dot{v}_{1i})|, \tag{37}$$

$$x_{2i}\dot{x}_{2i} \leq -\frac{x_{2i}^2}{\tau_{2i}} + x_{2i}^2 + \frac{1}{4}g_{2i}^2. \tag{38}$$

Taking the expectation of $\dot{V}_{2i}$ is similar to $\mathbb{E}\{\dot{V}_{1i}\}$,and we have $\mathbb{E}\{\dot{V}_{2i}\} = \dot{V}_{2i}$.

$$\begin{aligned}
\mathbb{E}\{\dot{V}_{2i}\} \leq{}& -\left(h_{2i} + \frac{1}{4}\right)\beta_{2i} m_{2i}^2 + \beta_{2i}|m_{2i}|\left(|m_{3i}| - (\zeta_{3i} + 1)\right)\\
&- h_{1i}\beta_{1i} m_{1i}^2 + H_{2i} + \frac{1}{4}x_{2i}^2 + \frac{1}{4}x_{1i}^2.
\end{aligned} \tag{39}$$

Procedure 3: The actual control input $u_i(t)$ is designed to stabilize the complete system, which encompasses all error variables. An event-triggered control scheme under DoS attacks is proposed as follows:

$$u_i(t) = W_i(t_k^i), \quad \forall t \in [t_k^i, t_{k+1}^i). \tag{40}$$

With the DoS attacks, the $u_i(t)$ is expressed as

$$u_i^d(t) = \alpha_i(t) u_i(t). \tag{41}$$

Define the next triggering instant t_{k+1}^i as the first time t after t_k^i satisfying

$$|W_i(t) - u_i(t)| \geq \begin{cases} \hat{\eta}_i + \delta_i|u_i(t)|, & \text{if } |u_i(t)| < N_i \\ \eta_i, & \text{otherwise} \end{cases} \tag{42}$$

where η_i and $\hat{\eta}_i$ are positive constants, $0 < \delta_i < 1$, and t_k^i indicates the k-th event time for vehicle i.

Remark 3: The event-triggered mechanism adaptively adjusts two thresholds to reduce update frequency under DoS attacks. Their selection reflects a trade-off between communication efficiency and control performance, and the values used here are determined by simulation to minimize unnecessary communication while preserving stability.

The derivative of m_{3i} is computed, and the RBFNN employed to approximate the nonlinear uncertain term as follows:

$$\begin{aligned}
\dot{m}_{3i} &= \dot{a}_i - \dot{\rho}_{2i}\\
&= u_i^d + f_i(p_i(t), a_i(t), v_i(t)) - \dot{\rho}_{2i}\\
&= \alpha_i u_i + W_i^{*T} S_i(Z_i)
\end{aligned} \tag{43}$$

where $S_i(Z_i) = [s_1(Z_i),\ s_2(Z_i),\ \ldots,\ s_n(Z_i),\ 1]^T$ is the RBF basis function vector, with $Z_i = [p_i,\ a_i,\ v_i,\ \dot{\omega}_{2i}]^T$ as the input. The vector $W_i^* = [w_{1i}, \ldots, w_{ni}, \epsilon_i(t)]^T$ comprises n neural weights, where $\epsilon_i(t)$ characterizes the error in approximating $f_i(p_i, a_i, v_i)$ by $\dot{\rho}_{2i}$.

Remark 4: In this framework, the vehicle dynamics are not split into known and unknown parts; instead, the nonlinear function $f(p_i(t), v_i(t), a_i(t))$ is regarded as a lumped uncertainty. The RBFNN approximates and compensates this uncertainty online, while the remaining control law addresses the integrator dynamics. Thus, the adaptive RBFNN captures complex nonlinear behaviors, enabling robust control of the uncertain system.

The Lyapunov candidate function is selected as follows:

$$V_{3i} = \frac{1}{2}\beta_{3i} m_{3i}^2 + \frac{1}{2\gamma_i}\tilde{\theta}_i^2 + V_{2i}. \tag{44}$$

Here, $\tilde{\theta} i = \hat{\theta} i - \theta_i$ denotes the estimation error, with $\theta_i = (\sigma^T\sigma^+\epsilon^2)^{1/2}$, where $\sigma^* = [w_{1i},\ w_{2i},\ \ldots,\ w_{ni}]^T$, $\hat{\theta}_i$ is the adaptive estimate of θ_i, and ϵ represents the prescribed approximation accuracy. Clearly, $|W_i^{*T} S_i(Z_i)|$ is upper-bounded by $\theta_i|S_i(Z_i)|$.

Case 1: For the case where $|u_i(t)| \geq N_i$, the adaptive control input and its associated parameter update law are formulated as

$$W_i(t) = \rho_{3i} - \bar{\eta}_i \tanh\left(\frac{X(m_{3i})\bar{\eta}_i}{\epsilon_i}\right), \tag{45}$$

$$\dot{\hat{\theta}}_i = \gamma_i \left(\beta_{3i} m_{3i} \psi_i - \sigma_i \hat{\theta}_i \right) \tag{46}$$

where $\bar{\eta}_i > \eta_i$, ϵ_i are positive designed parameters, $\psi_i = H(z_{3i}) \| S_i(Z_i) \|$ and ρ_{3i} is defined accordingly. The rationale for designing the adaptive control law is summarized as follows:

$$\rho_{3i} = -\frac{1}{\bar{\alpha}_d} \left((h_{3i}+1) m_{3i} + \hat{\theta}_i \psi_i \right) - 0.2785 X(z_{3i}) \epsilon_i. \tag{47}$$

Remark 5: The adaptive controller compensates nonlinear uncertainties through $\hat{\theta}_i \psi_i$ and avoids Zeno behavior by ensuring continuity of W_{3i} via the smooth function $X(m_{3i})$.

From the event-triggering condition (42), $|W_i(t) - u_i(t)| < \eta_i$ for $t \in (t_k^i, t_{k+1}^i)$. Hence, there exists $\lambda_i(t) \in (-1, 1)$ such that $u_i(t) = W_i(t) - \lambda_i(t)\eta_i$. Taking the expectation of $\dot{V}_{3i}$ then yields

$$\begin{aligned}
\mathbb{E}\{\dot{V}_{3i}\} &= \mathbb{E}\{\beta_{3i} m_{3i} \dot{m}_{3i}\} - \frac{1}{\gamma_i} \tilde{\theta}_i \dot{\hat{\theta}}_i + \mathbb{E}\{\dot{V}_{2i}\} \\
&\le \beta_{3i} m_{3i} \bar{\alpha}_d \left(W_i(t) - \lambda_i(t)\eta_i \right) + \beta_{3i} |m_{3i}| \theta_i \| S(Z_i) \| \\
&\quad + \frac{\tilde{\theta}_i \gamma_i}{\gamma_i} (\beta_{3i} m_{3i} \psi_i - \sigma_i \hat{\theta}_i) + \mathbb{E}\{\dot{V}_{2i}\} \\
&\le \beta_{3i} m_{3i} \bar{\alpha}_d \Bigg(-\frac{1}{\bar{\alpha}_d} \left((h_{3i}+1) m_{3i} + \hat{\theta}_i \psi_i \right) \\
&\quad - 0.2785 X(m_{3i}) \epsilon_i - \bar{\eta}_i \tanh \left(\frac{X(m_{3i}) \bar{\eta}_i}{\epsilon_i} \right) \\
&\quad - \lambda_i(t)\eta_i \Bigg) + \beta_{3i} m_{3i} \theta_i \psi_i + \beta_{3i} m_{3i} \tilde{\theta}_i \psi_i - \sigma_i \tilde{\theta}_i \hat{\theta}_i \\
&\quad + \mathbb{E}\{\dot{V}_{2i}\} \\
&\le -(h_{3i}+1) \beta_{3i} m_{3i}^2 - \beta_{3i} m_{3i} \psi_i (\hat{\theta}_i - \theta_i) - \sigma_i \tilde{\theta}_i \hat{\theta}_i \\
&\quad + \beta_{3i} m_{3i} \tilde{\theta}_i \psi_i + X(m_{3i}) \beta_{3i} |m_{3i}| \bar{\alpha}_d (-0.2785 X \\
&\quad (m_{3i}) \epsilon_i - \bar{\eta}_i \tanh \left(\frac{X(m_{3i}) \bar{\eta}_i}{\epsilon_i} \right) - \lambda_i(t)\eta_i) \\
&\quad + \mathbb{E}\{\dot{V}_{2i}\}
\end{aligned} \tag{48}$$

where $\Phi_1 = X(m_{3i}) \beta_{3i} |m_{3i}| \bar{\alpha}_d (-\bar{\eta}_i \tanh(\frac{X(m_{3i})\bar{\eta}_i}{\epsilon_i}) - 0.2785 X(m_{3i}) \epsilon_i - \lambda_i(t)\eta_i)$, $\tilde{\theta}_i = \hat{\theta}_i - \theta_i$, and substitude $\mathbb{E}\{\dot{V}_{2i}\}$.

$$\begin{aligned}
\mathbb{E}\{\dot{V}_{3i}\} &\le -(h_{3i}+1) \beta_{3i} m_{3i}^2 - (h_{2i} + \frac{1}{4}) \beta_{2i} m_{2i}^2 \\
&\quad - h_{1i} \beta_{1i} m_{1i}^2 + \beta_{2i} z_{2i}^2 (|m_{3i}| - (\zeta_{3i}+1)) \\
&\quad - \sigma_i \tilde{\theta}_i \hat{\theta}_i + \frac{1}{4} x_{1i}^2 + \frac{1}{4} x_{2i}^2 + \Phi_i
\end{aligned} \tag{49}$$

where $H_{3i} = \frac{1}{4} \beta_{2i} m_{2i}^2 + \beta_{2i} |m_{2i}| (|m_{3i}| - (\zeta_{3i}+1)) - \beta_{3i} m_{3i}^2$.

$$\begin{aligned}
\mathbb{E}\{\dot{V}_{3i}\} &\le -h_{3i} \beta_{3i} m_{3i}^2 - h_{2i} \beta_{2i} m_{2i}^2 - h_{1i} \beta_{1i} m_{1i}^2 \\
&\quad - \sigma_i \tilde{\theta}_i \hat{\theta}_i + \frac{1}{4} x_{1i}^2 + \frac{1}{4} x_{2i}^2 + \Phi_i + H_{3i}.
\end{aligned} \tag{50}$$

By similar reasoning as for H_{2i}, it follows that $H_{3i} \le 0$.

Defining

$$\begin{aligned}
\chi_i &= -\bar{\eta}_i \tanh \left(\frac{X(m_{3i}) \bar{\eta}_i}{\epsilon_i} \right) \\
&\quad - 0.2785 X(m_{3i}) \epsilon_i - \lambda_i(t) \eta_i
\end{aligned} \tag{51}$$

and applying Lemma 3, we have

- For $X(m_{3i}) = 1, \beta_{3i} = 1$, $\chi_i \le 0$, thus $\Phi_1 \le 0$.
- For $X(m_{3i}) = -1, \beta_{3i} = 1$, $\chi_i \ge 0$, thus $\Phi_1 \le 0$.
- For $X(m_{3i}) \in (-1, 1), \beta_{3i} = 0$, thus $\Phi_1 = 0$.

Therefore, $\Phi \le 0$ holds. Then we have

$$\begin{aligned}
\mathbb{E}\{\dot{V}_{3i}\} &\le -h_{1i} \beta_{1i} m_{1i}^2 - h_{2i} \beta_{2i} m_{2i}^2 - h_{3i} \beta_{3i} m_{3i}^2 \\
&\quad - \sigma_i \tilde{\theta}_i \hat{\theta}_i + \frac{1}{4} x_{1i}^2 + \frac{1}{4} x_{2i}^2.
\end{aligned} \tag{52}$$

Case 2: For the case where $|u_i(t)| < N_i$, the adaptive control law and corresponding parameter adaptation rule are constructed as follows:

$$\begin{aligned}
W_i(t) &= -(1+\delta_i) \Bigg(\tilde{\eta}_i \tanh \left(\frac{X(m_{3i}) \tilde{\eta}_i}{\epsilon_i} \right) \\
&\quad + \rho_{3i} \tanh \left(\frac{X(m_{3i}) \rho_{3i}}{\epsilon_i} \right) \Bigg),
\end{aligned} \tag{53}$$

$$\dot{\hat{\theta}}_i = \gamma_i \left(\beta_{3i} m_{3i} \psi_i - \sigma_i \hat{\theta}_i \right) \tag{54}$$

and

$$\rho_{3i} = -\frac{1}{\bar{\alpha}_d} \left((h_{3i}+1) m_{3i} + \hat{\theta}_i \psi_i \right) - 0.557 X(m_{3i}) \epsilon_i \tag{55}$$

where $\tilde{\eta}_i > \hat{\eta}_i$.

Based on the event-triggering mechanism, the inequality $|W_i(t) - u_i(t)| < \hat{\eta}_i + \delta_i |u_i(t)|$ is satisfied for all $t \in (t_k^i, tk+1^i)$. Consequently, there exist two time-varying parameters $|\bar{\lambda}_i(t)| \le 1$ and $|\hat{\lambda}_i(t)| \le 1$, such that $W_i(t) = (1 + \bar{\lambda}_i(t)\delta_i) u_i(t) + \hat{\lambda}_i(t) \hat{\eta}_i$. This leads to the following expression for the control input: $u_i(t) = \frac{W_i(t)}{1+\bar{\lambda}_i(t)\delta_i} - \frac{\hat{\lambda}_i(t)\hat{\eta}_i}{1+\bar{\lambda}_i(t)\delta_i}$. Taking the mathematical expectation of the time derivative of the Lyapunov function V_{3i}, we derive the following result:

$$\begin{aligned}
\mathbb{E}\{\dot{V}_{3i}\} &\le \beta_{3i} m_{3i} \bar{\alpha}_d \left(\frac{W_i(t)}{1+\bar{\lambda}_i \delta_i} - \frac{\hat{\lambda}_i(t) \hat{\eta}_i}{1+\bar{\lambda}_i(t)\delta_i} \right) + \mathbb{E}\{\dot{V}_{2i}\} \\
&\quad + \frac{\tilde{\theta}_i \gamma_i}{\gamma_i} (\beta_{3i} m_{3i} \psi_i - \sigma_i \hat{\theta}_i) + \beta_{3i} |m_{3i}| \theta_i \| S(Z_i) \| \\
&\le \beta_{3i} m_{3i} \bar{\alpha}_d \Bigg(\frac{1+\delta_i}{1+\bar{\lambda}_i(t)\delta_i} \Bigg(-\tilde{\eta}_i \tanh \left(\frac{X(m_{3i}) \tilde{\eta}_i}{\epsilon_i} \right) \\
&\quad - \rho_{3i} \tanh \left(\frac{X(m_{3i}) \rho_{3i}}{\epsilon_i} \right) \Bigg) + \left| \frac{X(m_{3i}) \hat{\lambda}_i(t) \hat{\eta}_i}{1+\bar{\lambda}_i(t)\delta_i} \right| \Bigg) \\
&\quad + \beta_{3i} m_{3i} \theta_i \psi_i + \beta_{3i} m_{3i} \tilde{\theta}_i \psi_i - \sigma_i \tilde{\theta}_i \hat{\theta}_i + \mathbb{E}\{\dot{V}_{2i}\} \\
&\le \beta_{3i} m_{3i} \bar{\alpha}_d \Bigg(\frac{1+\delta_i}{1+\bar{\lambda}_i(t)\delta_i} \Bigg(0.557 \epsilon_i - \frac{1}{\bar{\alpha}_d} \Big((h_{3i}+1) \\
&\quad m_{3i} + \hat{\theta}_i \psi_i \Big) - 0.557 X(m_{3i}) \epsilon_i \Bigg) \Bigg) + \beta_{3i} m_{3i} \bar{\alpha}_d
\end{aligned}$$

$$\left(\left|\frac{\hat{\eta}_i}{1+\bar{\lambda}_i(t)\delta_i}\right| - \frac{1+\delta_i\tilde{\eta}_i}{1+\bar{\lambda}_i(t)\delta_i}\right) + \beta_{3i}m_{3i}\theta_i\psi_i$$
$$+ \beta_{3i}m_{3i}\tilde{\theta}_i\psi_i - \sigma_i\tilde{\theta}_i\hat{\theta}_i + \mathbb{E}\{\dot{V}_{2i}\}$$
$$\leq -(h_{3i}+1)\beta_{3i}m_{3i}^2 - \beta_{3i}m_{3i}\hat{\theta}_i + \beta_{3i}m_{3i}\theta_i\psi_i$$
$$+ \beta_{3i}m_{3i}\tilde{\theta}_i\psi_i - \sigma_i\tilde{\theta}_i\hat{\theta}_i + \mathbb{E}\{\dot{V}_{2i}\}. \tag{56}$$

Substitute $\mathbb{E}\{\dot{V}_{2i}\}$ and where $H_{3i} = \frac{1}{4}\beta_{2i}m_{2i}^2 + \beta_{2i}|m_{2i}|(|m_{3i}| - (\zeta_{3i}+1)) - \beta_{3i}m_{3i}^2$, similar to Case1:

$$\mathbb{E}\{\dot{V}_{3i}\} \leq -h_{1i}\beta_{1i}m_{1i}^2 - h_{2i}\beta_{2i}m_{2i}^2 - h_{3i}\beta_{3i}m_{3i}^2$$
$$- \sigma_i\tilde{\theta}_i\hat{\theta}_i + \frac{1}{4}x_{1i}^2 + \frac{1}{4}x_{2i}^2. \tag{57}$$

Consider the following compact set:

$$\mathbf{\Omega} = \left\{[\bar{m}_1, \bar{m}_2, \bar{m}_3, \bar{x}_1, \bar{x}_2, \bar{\hat{\theta}}] : V \leq p\right\} \subset \mathbb{R}^{6N} \tag{58}$$

where $\bar{m}_k = [m_{k1}, \ldots, m_{kN}]^T$ for $k = 1, 2, 3$, $\bar{\hat{\theta}} = [\hat{\theta}_1, \ldots, \hat{\theta}_N]^T$, and $\bar{x}_{k'} = [x_{k'1}, \ldots, x_{k'N}]^T$ for $k' = 1, 2$. A suitable Lyapunov function is then constructed over this set.

$$V = \sum_{j=1}^{N}\left(V_{3j} + \frac{1}{2}x_{1j}^2 + \frac{1}{2}y_{xj}^2\right). \tag{59}$$

Compactness of $\mathbf{\Omega}_i$ and $\mathbf{\Omega}$ with $V \leq p$ ensures bounded m_{ki}, $x_{k'i}$, $\hat{\theta}_i$, and auxiliary variables, while g_{1i}^2 and g_{2i}^2 attain finite maxima M_{1i}, M_{2i}.

B. Analysis of Stability With Distributed Strategy

Under the event-triggering mechanism in (42), the platoon applies the distributed controller (40) (derived from (45), (47), (53), and (55)) together with the estimator parameter update law (46). Assume $V(0) \leq p$ with $p > 0$, and that the design parameters satisfy the following for all $i \in \mathcal{N}$,

$$h_{1i},\, h_{2i},\, h_{3i} \geq a_0, \quad \frac{1}{\tau_{1i}},\, \frac{1}{\tau_{2i}} \geq a_0 + \frac{5}{4} \tag{60}$$

where

$$a_0 = \min_{i\in\mathcal{N}}\left\{h_{1i},\, h_{2i},\, h_{3i},\, \frac{1}{2}\sigma_i,\, \frac{1}{\tau_{1i}} - \frac{5}{4},\, \frac{1}{\tau_{2i}} - \frac{5}{4}\right\}. \tag{61}$$

Remark 6: The conditions in (60) and (61) serve as controller design guidelines rather than strict physical assumptions, ensuring convergence through parameter tuning. These parameters involve trade-offs: larger gains speed convergence but risk overshoot and noise sensitivity, smaller filter constants enhance tracking but amplify high-frequency disturbances, and the adaptive gain must balance nonlinear approximation speed with weight-update stability.

Theorem 1: Under Assumptions 1–2, the proposed strategy achieves practical consensus in position and velocity, excludes Zeno behavior, and ensures string stability under both BD and TPF topologies.

Proof: By combining the equation below with (57) and (59),

$$\sigma_i\tilde{\theta}_i\hat{\theta}_i = \sigma_i(\tilde{\theta}_i\theta_i - \tilde{\theta}_i^2)$$
$$\leq \sigma_i\left(\frac{1}{2}(\tilde{\theta}_i^2 + \theta_i^2) - \tilde{\theta}_i^2\right)$$
$$= -\frac{1}{2}\sigma_i\tilde{\theta}_i^2 + \frac{1}{2}\sigma_i\theta_i^2 \tag{62}$$

and taking the expectation of $\dot{V}$, we obtain that

$$\mathbb{E}\{\dot{V}\} = \sum_{i=1}^{N}\left(\mathbb{E}\{\dot{V}_{3i}\} + x_{1i}\dot{x}_{1i} + x_{2i}\dot{x}_{2i}\right)$$
$$\leq \sum_{i=1}^{N}\Bigg(-h_{1i}m_{1i}^2 - h_{2i}m_{2i}^2 - h_{3i}m_{3i}^2$$
$$- \left(\frac{1}{\tau_{1i}} - \frac{5}{4}\right)x_{1i}^2 + \frac{1}{4}M_{1i} - \left(\frac{1}{\tau_{2i}} - \frac{5}{4}\right)x_{2i}^2$$
$$+ \frac{1}{4}M_{2i} - \frac{1}{2}\sigma_i\tilde{\theta}_i^2 + \frac{1}{2}\sigma_i\theta_i^2\Bigg). \tag{63}$$

From (59) and (63), we have

$$\mathbb{E}\{\dot{V}\} \leq -\alpha_0 V + \mu \tag{64}$$

where $\mu = \sum_{i=1}^{N}(\frac{1}{2}\sigma_i\theta_i^2 + \frac{1}{4}M_{1i} + \frac{1}{4}M_{2i})$. By Grönwall's inequality and Lemma 5, it follows that

$$0 \leq \mathbb{E}\{V(t)\} \leq \frac{\mu}{\alpha_0}(1 - e^{-\alpha_0 t}) + V(0)e^{-\alpha_0 t}. \tag{65}$$

■

Thus, $m_i(t)$ and $\tilde{\theta}_i$ are uniformly bounded for all $i \in \mathcal{N}$, implying bounded $\hat{\theta}_i$. Moreover, $|m_{1i}|$ can be made arbitrarily small as $t \to \infty$ with appropriate controller gains.

Defining $\bar{m}_1 = (\mathcal{L} + \mathcal{K})$ with $p = [p_1 - p_0 + d_{10}, \ldots, p_N - p_0 - d_{N-1,0}]^T$ and noting $\lambda_{\min}(\mathcal{L} + \mathcal{K}) > 0$, the spacing error $|p_i - p_{i-1} - l_{i-1} - y_i^d|$ can be made arbitrarily small, ensuring practical position consensus; velocity consensus follows similarly. The event-triggered mechanism is Zeno-free since $E_i(t) = W_i(t) - u_i(t)$ has bounded derivative, guaranteeing a strictly positive inter-event time.

String stability is guaranteed for both BD and TPF topologies. For the BD topology, the stability condition is $|(L_i - L_i^d) - p(L_{i+1} - L_{i+1}^d)| \leq \digamma_i$ with parameter $p > 1$. For the TPF topology, the condition is $|q(L_{i-1} - L_{i-1}^d) - (L_i - L_i^d)| \leq \bar{\digamma}_i$ with parameter $q \in (0, 1)$. The bounds $\digamma_i$ and $\bar{\digamma}_i$ are tunable and can be made arbitrarily small. In both scenarios, the error does not amplify along the platoon, as shown by

$$\left|\frac{L_i - L_i^d}{L_{i+1} - L_{i+1}^d}\right| \geq 1. \tag{66}$$

Therefore, string stability of the platoon is guaranteed.

Remark 7: To prevent Zeno behavior, a strictly positive lower bound on $|\dot{u}_i(t)|$ is required. Since $|\dot{u}_i(t)|$ depends on possibly discontinuous acceleration derivatives, a first-order filter is introduced to guarantee Zeno-freeness.

An algorithm is developed for the synthesis of adaptive distributed event-triggered controllers.

Algorithm 1: Event-Triggered Adaptive Control with RBFNN under DoS Attacks.

Initialize: vehicle states, RBF weights $\hat{\theta}_i$, filters κ_1, κ_2, control memory $u_{\text{prev},i} \leftarrow 0$
for each time step k **do**
  Update leader vehicle state
  for each follower $i = 1, \ldots, N$ **do**
    Compute errors m_{1i}, m_{2i}, m_{3i} from neighbor states ▷Backstepping coordinates
    Derive control law $W_i(t)$ with RBFNN compensation ▷Approximate nonlinearities
    if event-triggering condition (42) holds **then**
      $u_{\text{prev},i} \leftarrow W_i(t)$ ▷Transmit updated control
    end if
    Update RBF weights $\hat{\theta}_i$ via (46) ▷Online adaptation
    Apply DoS effect: $u_i \leftarrow \alpha_i(t) u_{\text{prev},i}$ ▷Bernoulli packet loss
  end for
end for

TABLE I
PARAMETER SETTINGS

Parameter	Value	Parameter	Value
h_{1i}, h_{2i}, h_{3i}	0.08	τ_{1i}, τ_{2i}	0.08
$\eta_i, \hat{\eta}_i$	0.0005, 0.0004	$\bar{\eta}_i, \tilde{\eta}_i$	0.005, 0.004
δ_i	0.02	N_i	1
ε_i	0.5	γ_i	0.3
σ_i	0.015		

IV. SIMULATION

To validate the proposed method under representative scenarios, both BD and TPF topologies are considered, where BD provides richer information and TPF relies on less. Simulations are conducted in MATLAB R2024a under the BD topology for a four-vehicle platoon under stochastic DoS attacks, while the theoretical results apply to both, ensuring generality.

A 4-dimensional RBF network with 12 Gaussian basis functions (uniform centers, width $\sigma = 1$) is employed, providing a balance between approximation accuracy and efficiency within the compact set. The number of 12 basis functions was empirically determined to ensure adequate coverage of the input space without redundancy. The communication weights are set as $a_{ij} = 1.1$ for $i > j$ and $a_{ij} = 1$ for $i < j$, with $\text{diag}\{1, 0, \ldots, 0\}$. The resulting matrix $\mathcal{L} + \mathcal{K}$ is given by:

$$\mathcal{L} + \mathcal{K} = \begin{bmatrix} 2.1 & -1.1 & & & \\ -1 & 2.1 & -1.1 & & \\ & -1 & 2.1 & -1.1 & \\ & & -1 & 2.1 & -1.1 \\ & & & -1 & 1 \end{bmatrix} \tag{67}$$

Under the parameter constraints summarized in Table I, the numerical results shown in Figs. 2–7 collectively substantiate the effectiveness of the proposed adaptive distributed eventtriggered

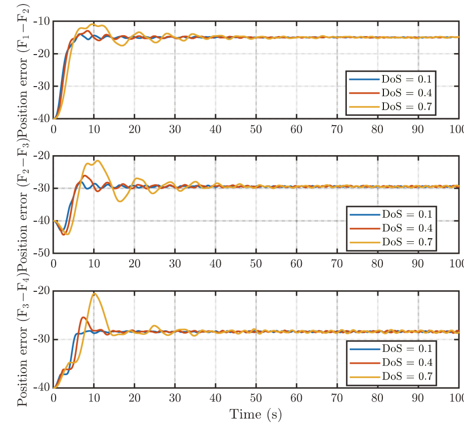

Fig. 2. Neighboring positional errors under DoS attacks.

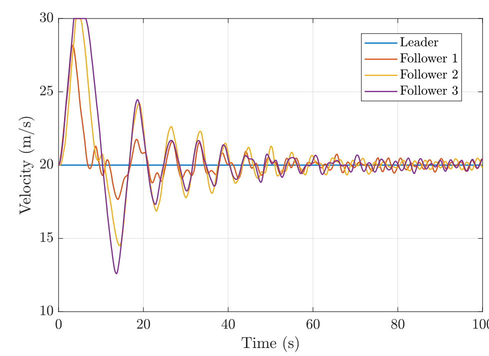

Fig. 3. The velocities of leader and followers.

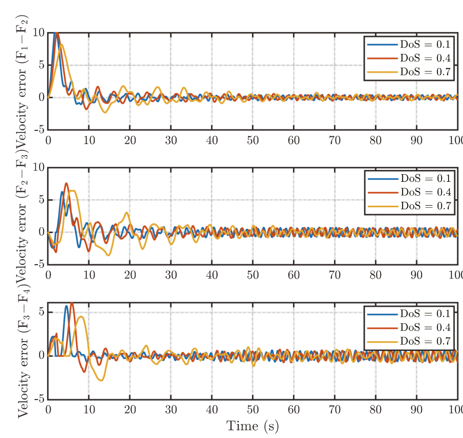

Fig. 4. Neighboring velocity errors under DoS attacks.

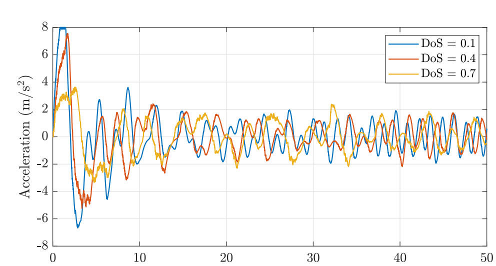

Fig. 5. Leader and first follower acceleration under DoS attacks.

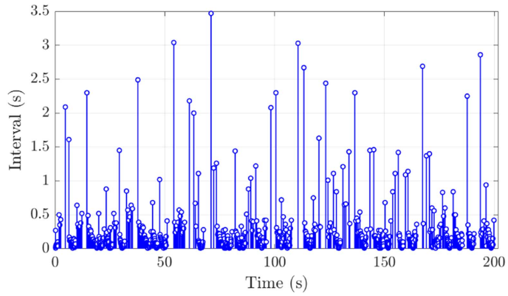

Fig. 6. Event-triggered intervals of the 1st follower.

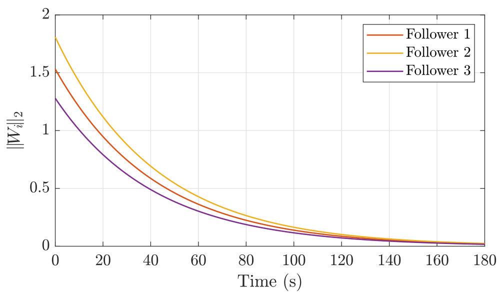

Fig. 7. The variation in the weight values of following vehicles.

control framework in achieving practical position–velocity consensus in two domains. Fig. 2 further shows that the peak position errors for three attack levels (DoS $= 0.1, 0.4, 0.7$) are bounded within ± 10 m and converge to ± 0.5 m in 6 s, satisfying the stringstability criterion$\|L_i(t) - L_i^d(t)\| \leq \Delta_1$ and thereby guaranteeing that the intervehicular safety distance is preserved.

As illustrated in Fig. 3, all vehicle speeds synchronize to 25 ms^{-1} within 15 s, and, as Fig. 4 shows, the velocity error drops from ≤ 0.4 to < 0.05 ms^{-1} within 3 s, satisfying the consensus bound $\|v_i - v_{i-1}\| \leq \Delta_2$.

Fig. 5 further indicates that, even at a 0.7 attack rate, acceleration mismatch is confined to $\pm 8\mathrm{ms}^{-2}$ and disappears by 8 s, confirming that backstepping compensation suppresses actuator saturation. Fig. 6 shows update intervals stay within 0.6–1.2 s without dense triggering, cutting communication load and avoiding Zeno behaviour, while Fig. 7 demonstrates the RBFNN weight norms stabilise below 2 at approximately 100s, matching the exponential decay law $\dot{\hat{\theta}}_i = \gamma_i(\beta_{3i} m_{3i} \psi_i - \sigma_i \hat{\theta}_i)$ and indicating adequate nonlinear approximation. Fig. 8 shows the velocity responses of the conventional control system under a DoS attack with intensity 0.4. The velocity error between the leader and the first follower exhibits persistent oscillations of about $\pm 4\mathrm{ms}^{-1}$ without attenuation over 200 seconds, indicating a lack of string stability.

In summary, under stochastic DoS attack probabilities between 0.1 and 0.7, the proposed control framework sustains precise tracking, preserves platoon stability, and minimizes communication overhead, thereby demonstrating superior robustness and strong engineering applicability.

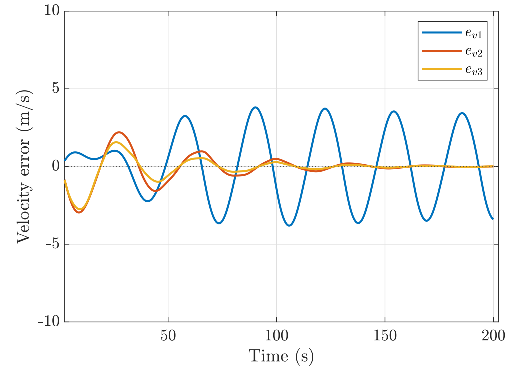

Fig. 8. Neighboring velocity errors with DoS in conventional control.

V. Conclusion

To control nonlinear vehicle platoons under stochastic DoS attacks, we propose an online RBFNN-enhanced adaptive, distributed backstepping framework. Stability is maintained while redundant transmissions are reduced via a dual-mode, Zeno-free event-triggering mechanism. Lyapunov analysis and extensive simulations confirm string stability and practical consensus for BD and TPF topologies across varied attack intensities. Looking ahead, potential applications include C-ACC, coordinated ramp merging, and eco-platooning in V2X-constrained ITS; theoretically, a natural next step is to handle switching directed graphs with delays/losses and establish ISS-based guarantees, alongside HIL or large-scale field tests to validate scalability.

References

[1] Z. Xiao, J. Shu, H. Jiang, G. Min, H. Chen, and Z. Han, "Overcoming occlusions: Perception task-oriented information sharing in connected and autonomous vehicles," *IEEE Netw.*, vol. 37, no. 4, pp. 224–229, Jul.–Aug. 2023.

[2] C. Liu, Z. Xiao, W. Long, T. Li, H. Jiang, and K. Li, "Vehicle trajectory data processing, analytics, and applications: A survey," *ACM Comput. Surv.*, vol. 57, no. 9, pp. 1–36, May 2025.

[3] Z. Xiao, J. Shu, H. Jiang, G. Min, H. Chen, and Z. Han, "Perception task offloading with collaborative computation for autonomous driving," *IEEE J. Sel. Areas Commun.*, vol. 41, no. 2, pp. 457–473, Feb. 2023.

[4] X. Ge, Q.-L. Han, X.-M. Zhang, and D. Ding, "Communication resource-efficient vehicle platooning control with various spacing policies," *IEEE/CAA J. Automatica Sinica*, vol. 11, no. 2, pp. 362–376, Feb. 2024.

[5] Z. Xiao, J. Shu, H. Jiang, G. Min, J. Liang, and A. Iyengar, "Toward collaborative occlusion-free perception in connected autonomous vehicles," *IEEE Trans. Mobile Comput.*, vol. 23, no. 5, pp. 4918–4929, May 2024.

[6] H. Hasan, F. A. Samman, and M. Anshar, "Trajectory tracking of autonomous vehicle that uses state feedback linearization with ackerman method and observer feedback," in *Proc. 5th Int. Seminar Res. Inf. Technol. Intell. Syst.*, Dec. 2022, pp. 191–197.

[7] L. Martins, C. Cardeira, and P. Oliveira, "Feedback linearization with zero dynamics stabilization for quadrotor control," *J. Intell. Robot. Syst.*, vol. 101, pp. 1–17, Dec. 2021.

[8] C. Zhao, X. Duan, L. Cai, and P. Cheng, "Vehicle platooning with non-ideal communication networks," *IEEE Trans. Veh. Technol.*, vol. 70, no. 1, pp. 18–32, Jan. 2021.

[9] D. Liu, B. Besselink, S. Baldi, W. Yu, and H. L. Trentelman, "Output-feedback design of longitudinal platooning with adaptive disturbance decoupling," *IEEE Control Syst. Lett.*, vol. 6, pp. 3104–3109, 2022.

[10] Z. Zhu, X. Tang, Y. Qin, Y. Huang, and E. Hashemi, "A survey of lateral stability criterion and control application for autonomous vehicles," *IEEE Trans. Intell. Transp. Syst.*, vol. 24, no. 10, pp. 10382–10399, Oct. 2023.

[11] S.-H. Lee, "A spatiotemporal spacing policy and string stability for heterogeneous vehicle platooning," *IEEE Trans. Veh. Technol.*, vol. 73, no. 11, pp. 16328–16340, Nov. 2024.

[12] Y. Zhu and F. Zhu, "Distributed adaptive longitudinal control for uncertain third-order vehicle platoon in a networked environment," *IEEE Trans. Veh. Technol.*, vol. 67, no. 10, pp. 9183–9197, Oct. 2018.

[13] S. Yu, C. Shen, and T. Ersal, "Autonomous driving using linear model predictive control with a Koopman operator based bilinear vehicle model," *IFAC-Papersonline*, vol. 55, no. 24, pp. 254–259, Oct. 2022.

[14] J. Wei, Y.-J. Liu, H. Chen, and L. Liu, "Fuzzy adaptive control for vehicular platoons with constraints and unknown dead-zone input," *IEEE Trans. Intell. Transp. Syst.*, vol. 24, no. 4, pp. 4403–4412, Apr. 2023.

[15] G. Chen, Q. Zhou, H. Ren, and H. Li, "Sensor-fusion-based event-triggered following control for nonlinear autonomous vehicles under sensor attacks," *IEEE Trans. Autom. Sci. Eng.*, vol. 22, pp. 17411–17420, 2025.

[16] S. Xiao, X. Ge, Q.-L. Han, and Y. Zhang, "Secure distributed adaptive platooning control of automated vehicles over vehicular ad-hoc networks under denial-of-service attacks," *IEEE Trans. Cybern.*, vol. 52, no. 11, pp. 12003–12015, Nov. 2022.

[17] C. Liu, Z. Xia, and R. J. Patton, "Distributed fault-tolerant consensus control of vehicle platoon systems with DoS attacks," *IEEE Trans. Veh. Technol.*, vol. 73, no. 10, pp. 14438–14449, Oct. 2024.

[18] X. Ge, Q.-L. Han, J. Wang, and X.-M. Zhang, "Scalable and resilient platooning control of cooperative automated vehicles," *IEEE Trans. Veh. Technol.*, vol. 71, no. 4, pp. 3595–3608, Apr. 2022.

[19] D. Zhang, Y.-P. Shen, S.-Q. Zhou, X.-W. Dong, and L. Yu, "Distributed secure platoon control of connected vehicles subject to DoS attack: Theory and application," *IEEE Trans. Syst., Man, Cybern. Syst.*, vol. 51, no. 11, pp. 7269–7278, Nov. 2021.

[20] J. Liu, Y. Dong, L. Zha, X. Xie, and E. Tian, "Reinforcement learning-based tracking control for networked control systems with DoS attacks," *IEEE Trans. Inf. Forensics Secur.*, vol. 19, pp. 4188–4197, 2024.

[21] Q. Jia, G. Li, D. Yu, C. K. Ahn, and C. Zhang, "Learning Chebyshev neural network-based spacecraft attitude tracking control ensuring finite-time prescribed performance," *Aerosp. Sci. Technol.*, vol. 148, Mar. 2024, Art. no. 109085.

[22] J. Wang, C. Wang, Y. Wei, and C. Zhang, "Observer-based neural formation control of leader–follower AUVs with input saturation," *IEEE Syst. J.*, vol. 15, no. 2, pp. 2553–2561, Jun. 2021.

[23] Y. Liu, D. Yao, H. Li, and R. Lu, "Distributed cooperative compound tracking control for a platoon of vehicles with adaptive NN," *IEEE Trans. Cybern.*, vol. 52, no. 7, pp. 7039–7048, Jul. 2022.

[24] J. Sun, J. Yang, S. Li, and Z. Zeng, "Predictor-based periodic event-triggered control for dual-rate networked control systems with disturbances," *IEEE Trans. Cybern.*, vol. 52, no. 8, pp. 8179–8190, Aug. 2022.

[25] J. Liu, N. Zhang, Y. Li, X. Xie, E. Tian, and J. Cao, "Learning-based event-triggered tracking control for nonlinear networked control systems with unmatched disturbance," *IEEE Trans. Syst., Man, Cybern. Syst.*, vol. 53, no. 5, pp. 3230–3240, May 2023.

[26] J. Sun, J. Yang, W. X. Zheng, and S. Li, "Periodic event-triggered control for a class of nonminimum-phase nonlinear systems using dynamic triggering mechanism," *IEEE Trans. Circuits Syst. I, Reg. Papers*, vol. 69, no. 3, pp. 1302–1311, Mar. 2022.

[27] M. Wang, C. Zhao, J. Xia, and J. Sun, "Periodic event-triggered robust distributed model predictive control for multiagent systems with input and communication delays," *IEEE Trans. Ind. Informat.*, vol. 19, no. 11, pp. 11216–11228, Nov. 2023.

[28] B. Hu, "Stochastic stability analysis for vehicular networked systems with state-dependent bursty fading channels: A self-triggered approach," *Automatica*, vol. 123, Jan. 2021, Art. no. 109352.

[29] L. Zhang, J. Sun, and Q. Yang, "Distributed model-based event-triggered leader–follower consensus control for linear continuous-time multiagent systems," *IEEE Trans. Syst., Man, Cybern. Syst.*, vol. 51, no. 10, pp. 6457–6465, Oct. 2021.

[30] X. Ge, Q.-L. Han, L. Ding, Y.-L. Wang, and X.-M. Zhang, "Dynamic event-triggered distributed coordination control and its applications: A survey of trends and techniques," *IEEE Trans. Syst., Man, Cybern. Syst.*, vol. 50, no. 9, pp. 3112–3125, Sep. 2020.

[31] G. Wu, G. Chen, H. Zhang, and C. Huang, "Fully distributed event-triggered vehicular platooning with actuator uncertainties," *IEEE Trans. Veh. Technol.*, vol. 70, no. 7, pp. 6601–6612, Jul. 2021.

[32] J. Lan, D. Zhao, and D. Tian, "Data-driven robust predictive control for mixed vehicle platoons using noisy measurement," *IEEE Trans. Intell. Transp. Syst.*, vol. 24, no. 6, pp. 6586–6596, Jun. 2023.

[33] J. J. R. Liu, K.-W. Kwok, Y. Cui, J. Shen, and J. Lam, "Consensus of positive networked systems on directed graphs," *IEEE Trans. Neural Netw. Learn. Syst.*, vol. 33, no. 9, pp. 4575–4583, Sep. 2022.

[34] G. Difilippo, M. P. Fanti, and A. M. Mangini, "Maximizing convergence speed for second order consensus in leaderless multi-agent systems," *IEEE/CAA J. Automatica Sinica*, vol. 9, no. 2, pp. 259–269, Feb. 2022.

[35] S. Feng, A. Cetinkaya, H. Ishii, P. Tesi, and C. D. Persis, "Networked control under DoS attacks: Tradeoffs between resilience and data rate," *IEEE Trans. Autom. Control*, vol. 66, no. 1, pp. 460–467, Jan. 2021.

[36] I. Herman, D. Martinec, Z. Hurák, and M. Sebek, "Scaling in bidirectional platoons with dynamic controllers and proportional asymmetry," *IEEE Trans. Autom. Control*, vol. 62, no. 4, pp. 2034–2040, Apr. 2017.

[37] V. E. Ismailov, "A three layer neural network can represent any multivariate function," *J. Math. Anal. Appl.*, vol. 523, no. 1, Jul. 2023, Art. no. 127096.

[38] M. M. Polycarpou and P. A. Ioannou, "A robust adaptive nonlinear control design," *Automatica*, vol. 32, no. 3, pp. 423–427, Jun. 1996.

[39] G. Wen, C. L. P. Chen, Y.-J. Liu, and Z. Liu, "Neural network-based adaptive leader-following consensus control for a class of nonlinear multiagent state-delay systems," *IEEE Trans. Cybern.*, vol. 47, no. 8, pp. 2151–2160, Aug. 2017.

[40] V. Vegamoor, S. Rathinam, and S. Darbha, "String stability of connected vehicle platoons under lossy v2v communication," *IEEE Trans. Intell. Transp. Syst.*, vol. 23, no. 7, pp. 8834–8845, Jul. 2022.

[41] J. Zhou, C. Wen, and Y. Zhang, "Adaptive backstepping control of a class of uncertain nonlinear systems with unknown backlash-like hysteresis," *IEEE Trans. Autom. Control*, vol. 49, no. 10, pp. 1751–1759, Oct. 2004.

Xiaoping Zhao received the Ph.D. degree in measurement technology and instruments from the Institute of Vibration Engineering, School of Astronautics, Nanjing University of Aeronautics and Astronautics, Nanjing, China, in March 2009. From 2015 to 2015, she was a Visiting Scholar with the New Jersey Institute of Technology, Newark, NJ, USA. Since Apr. 2009, she has been with the School of Computer and Software, Nanjing University of Information Science and Technology, Nanjing, China, where she is currently an Associate Professor.

Junyao Ma received the B.S. degree in software engineering from Zijin College, Nanjing University of Science and Technology, Nanjing, China, in 2024. She is currently working toward the M.S. degree with the Nanjing University of Information Science and Technology, Nanjing. Her research interests include connected vehicle control systems, security control, and privacy protection.

Jinliang Liu (Senior Member, IEEE) received the Ph.D. degree in control theory and control engineering from the School of Information Science and Technology, Donghua University, Shanghai, China, in 2011. From 2013 to 2016, he was a Postdoctoral Research Associate with the School of Automation, Southeast University, Nanjing, China. From 2016 to 2017, he was a Visiting Researcher/Scholar with the Department of Mechanical Engineering, University of Hong Kong, Hong Kong. From 2017 to 2018, he was a Visiting Scholar with the Department of Electrical Engineering, Yeungnam University, Gyeongsan, South Korea. From 2011 to 2023, he was an Associate Professor and then a Professor with Nanjing University of Finance and Economics. In 2023, he joined the Nanjing University of Information Science and Technology, Nanjing, where he is currently a Professor with the School of Computer Science. His research interests include cyber-physical systems, unmanned systems, privacy preservation, and game theory.

Lijuan Zha (Senior Member, IEEE) received the Ph.D. degree in control science and engineering from Donghua University, Shanghai, China, in 2018. From 2017 to 2024, she was an Associate Professor with the College of Information Engineering, Nanjing University of Finance and Economics, Nanjing. From 2018 to 2023, she was a Postdoctoral Research Associate with the School of Mathematics, Southeast University, Nanjing. She is currently an Associate Professor with the College of Science, Nanjing Forestry University, Nanjing, China. Her research interests include networked control systems, neural networks, and complex dynamical systems.